Sulfonated Amphiphilic Block Copolymers: Synthesis, Self-Assembly in Water, and Application as Stabilizer in Emulsion Polymerization

Jiguang Zhang,[†] Matthew R. Dubay,[†] Carl J. Houtman,[‡] and Steven J. Severtson*,[†]

[†]*Department of Bioproducts and Biosystems Engineering, University of Minnesota, 2004 Folwell Avenue, St. Paul, Minnesota 55108, and* [‡]*USDA, Forest Products Laboratory, One Gifford Pinchot Drive, Madison, Wisconsin 53726*

ABSTRACT: Described is the synthesis of diblock copolymers generated via sequential atom transfer radical polymerization (ATRP) of poly(*n*-butyl acrylate) (P*n*BA) followed by chain augmentation with either sulfonated poly(2-hydroxyethyl methacrylate) (PHEMA) or poly(2-hydroxyethyl acrylate) (PHEA) blocks. ATRP of PHEMA or PHEA from P*n*BA macroinitiator was conducted in acetone/methanol 50:50 (v/v) and produced diblock copolymers of low PDI (< 1.3). Hydroxyl functional groups were converted to sulfonate through esterification using excess 2-sulfobenzoic acid cyclic anhydride (SBA). TEM images of aqueous block copolymer solutions reveal an array of polymer micelle morphologies including monodisperse spheres, cylinders, and cylinder aggregates. Surface tensions and critical micelle concentrations appear to be dependent more on hydrophile structure as opposed to its length. Application of the synthesized block copolymers as stabilizers for batch emulsion polymerization of *n*-butyl acrylate showed the polymeric surfactant effectively stabilizes latex particles and produces a lower polydispersity when compared with commonly applied commercial emulsifiers.

Introduction

Sulfonate or strong acid containing polymers have attracted significant research interest due to their potential use in a variety of applications including membranes for chemical separation, fuel cells, solid-state batteries, and biomineralization.[1−4] Given their versatile microphase separation behavior, which may have utility in lithium ion conductors and other notable applications, the amphiphilic block copolymer version is of particular interest.[5] However, direct sequential polymerization of such block copolymers has proved difficult for two major reasons. First, sulfonate monomers are incompatible with conventional anionic polymerization and most other controlled/living polymerization techniques and thus require postmodification of the precursor polymer or deprotection chemistry for preparation. For example, Leemans et al. reported the sequential anionic polymerization of methyl methacrylate (MMA) and glycidyl methacrylate followed by the modification of the glycidyl groups into sulfonate groups.[6] Second, even if the hydrophilic homopolymer block is generated in a controlled fashion, synthesis of the second, hydrophobic, block is greatly hindered by the solubility discrepancy of amphiphiles in a common solvent. As a result, sulfonate block copolymers have typically been generated through the use of protecting group chemistry or postmodification of precursor polymers such as sulfonation of a styrene precursor.[7,8]

With advancements in controlled radical polymerization techniques such as atom transfer radical polymerization (ATRP), reversible addition−fragmentation transfer (RAFT) polymerization, and nitroxide-mediated radical polymerization, the complexity of synthesizing block polymers, including strong acid forms, has been substantially reduced. For example, generation of various sulfonated polystyrene homopolymers has been demonstrated via direct polymerization of sodium styrenesulfonate

in aqueous media,[8−11] and direct synthesis of amphiphilic block polymers has also been reported by Masci et al.[12] Specifically, poly(potassium 3-sulfopropyl methacrylate)-*b*-PMMA copolymers were synthesized via ATRP in a water/dimethylformamide cosolvent.

In this paper, results are reviewed from a study on the synthesis and property characterization of strong acid block copolymers containing a hydrophobic block synthesized from *n*-butyl acrylate (*n*BA). Synthesis attempts using the approach described by Masci et al. were ineffective due to precipitation of the macroinitiator (MI) during polymerization of P*n*BA. This failure demonstrates an issue with regard to strong acid block copolymers; general synthesis strategies that do not rely on the solubility of monomers or multistep modifications are still absent from the literature. Alternative and more cumbersome approaches have shown success, but often with potential drawbacks. Garnier et al. reported the synthesis of a poly(2-acrylamido-2-methylpropanesulfonic acid)-*block*-P*n*BA via RAFT polymerization, but the polydispersity of the copolymer was not reported.[13] Synthesis of P*n*BA−poly(styrenesulfonate) starburst block copolymers was reported very recently via sequential ATRP of (P*n*BA) and poly(styrene) (PS) followed by the sulfonation of the PS blocks with sulfuric acid.[14] However, the harsh reaction conditions required for sulfonation tends to produce unwanted cross-linking of the final product or limits sulfonation.[4,15] Baek reported the synthesis of P*n*BA-*block*-poly(neopentyl *p*-styrenesulfonate) using sequential ATRP, but this required the deprotection of the neopentyl groups of the poly(neopentyl *p*-styrenesulfonate) block at a temperature greater than 170 °C.[15]

Recently, Vo and co-workers reported a benign synthesis route capable of producing homopolymers or zwitterionic sulfonated diblock copolymers via ATRP of hydroxyl-containing monomers followed by the esterification of the hydroxyl groups using 2-sulfobenzoic acid cyclic anhydride (SBA).[16] The sulfonated polymer maintained its narrow molecular weight distribution

*Corresponding author. E-mail: sever018@umn.edu.

after the esterification reaction. However, there have been no reports on the synthesis of amphiphilic block copolymers using this method. Here, Vo's method is adopted toward the synthesis of amphiphilic copolymers composed of a P*n*BA hydrophobic block and either a poly(hydroxyethyl acrylate) (PHEA) or a poly(hydroxyethyl methacrylate) (PHEMA) block sulfonated with SBA. Synthesis involves the ATRP of P*n*BA-*b*-PHEMA block copolymer in an acetone/methanol mixture followed by the esterification of PHEMA, as illustrated in Scheme 1. The degree of polymerization of the P*n*BA block ranges from 28 to nearly 1000 and the PHEMA block ranges from 39 to 67 while the molecular weight distribution (MWD) remains fairly narrow with polydispersity index (PDI) values less than 1.3.

This article is intended to be a detailed prelude describing the synthesis and viability of P*n*BA containing macrosurfactants to then be employed in a subsequent paper outlining their comparative enrichment effect in P*n*BA latex thin films and is organized as follows. First, the controlled polymerization of P*n*BA-SBA: PHEMA is described. The analysis of the resulting diblock copolymers via nuclear magnetic resonance (NMR), dynamic light scattering (DLS), transmission electron microscopy (TEM), size exclusion chromatography (SEC), confocal Raman spectroscopy, and tensiometry is then discussed. On the basis of these results, the amphiphilic behavior of the synthesized diblock copolymer in water is described. Finally, the subsequent batch emulsion polymerization reactions of *n*BA using the synthesized macrosurfactant with the highest molecular weight are outlined and discussed as a direct comparison to those employing the common commercial surfactant.

Experimental Section

Materials and Instruments. Methyl 2-bromopropionate (MBP, 98%, CAS No. 5445-17-0), copper(I) bromide (98%, CAS No. 7787-70-4), *N*,*N*,*N'*,*N''*,*N''*-pentamethyldiethylenetriamine (PMDETA, CAS No. 3030-47-5), 2,2'-bipyridine (CAS No. 366-18-7), acetic anhydride (CAS No. 108-24-7), 2-sulfobenzoic acid cyclic anhydride (SBA, ≥95%, CAS No. 81-08-3), triethylamine (TEA, CAS No. 121-44-8), potassium persulfate (CAS No. 7727-21-1), hydroxyethyl acrylate (HEA, 96%, CAS No. 818-61-1), hydroxyethyl methacrylate (HEMA, CAS No. 868-77-9), and *n*-butyl acrylate (*n*BA, CAS No. 141-32-2) were all obtained as high-purity reagent grade chemicals (≥99%, unless otherwise stated) from Sigma-Aldrich (St. Louis, MO) and used without further purification. All organic solvents were AR grade and were also purchased from Sigma-Aldrich. Disodium (nonylphenoxypolyethoxy) ethyl sulfosuccinate (Aerosol A-103) (NPE, CAS No. 9040-38-4) was obtained from CYTEC Industries, Inc. (West Paterson, NJ).

SEC analyses for the synthesized polymers were performed using a Waters (Milford, MA) 150-C Plus instrument equipped with a differential refractometer detector (Waters 410). Tetrahydrofuran (THF) was used as the eluent with a flow rate of 1.0 mL/min at 30 °C, and the system was calibrated using PS standards ranging from 600 to 380 000 g/mol. The sample preparation was performed with concentrations ranging from 1 to 20 mg/mL in THF. Prior to injection, samples were filtered through a membrane with a 0.45 μm pore size.

All ^{1}H NMR spectra were recorded in either CDCl$_3$, CD$_3$OD, or *d*$_6$-DMSO (Cambridge Isotope Laboratories, Andover, MA) solvents using a Varian (Palo Alto, CA) Unity 300 spectrometer (with a Varian Inova console) collecting 50 scans per spectrum.

The Raman spectroscopy capabilities of a 300R confocal Raman microscope equipped with a UHTS200 spectrometer and a DV401 CCD detector from WITec (Ulm, Germany) were utilized for the characterization of polymeric functional groups. More experimental details about the instrument setup and analysis can be found in previously published literature.[17]

Aqueous solutions (~0.1 wt %) of the block copolymer were characterized by TEM on a JEOL (Tokyo, Japan) 1210 microscope operating at 120 kV, allowing a direct visualization of the micellar morphologies. A drop of polymer solution filtered through a 0.45 μm PVDF Millipore filter was placed on a carbon-coated copper grid, excess liquid was removed, sample was dried, and 2% phosphotungstic acid (PTA) stain was applied. Uranyl acetate-stained TEM samples were prepared by placing a drop of polymer solution onto a carbon film-coated copper grid. About a half minute later, the excess liquid was removed. After a few minutes, a drop of 2 wt % uranyl acetate solution was placed on the grid and allowed to settle. Excess solution was then removed, and the sample was dried for at least 30 min in air before the TEM analysis.

Surface tension measurements were performed following the Wilhelmy plate method with a Krüss Model K100 tensiometer (Hamburg, Germany). Aqueous solutions of specific surfactant concentrations were vigorously stirred for at least 2 days prior to measurements in order to allow equilibrium to be reached. The surface tension of pure water was confirmed prior to each measurement and subsequent to each measurement. The platinum plate was washed with deionized water and acetone and flame-dried.

Dynamic light scattering measurements were conducted using a 90Plus particle size analyzer (Brookhaven Instruments Co., Holtsville, NY) measuring the 90° scattering intensity of a 658 nm incident laser beam at room temperature (23 °C). The NNLS software of the light scattering instrument was used to analyze the DLS data. The data were analyzed by the cumulant method to yield the average hydrodynamic diameter D_h and polydispersity (PD) K_1^2/K_2, where K_1 and K_2 denote the first- and second-order cumulants, respectively. More detailed descriptions of the calculation can be found in the literature.[18] All samples were filtered using a 0.45 μm PVDF Millipore filter, and reported PD values are an average of seven repeated measurements.

Synthesis of P*n*BA Macroinitiator (MI) via ATRP. In a typical synthesis, a 500 mL flask containing 200 g of *n*BA dissolved in acetone was sealed with a septum and purged with N$_2$ for at least 20 min. CuBr was then charged into the flask quickly. After 5 min, deaerated PMDETA was injected and the CuBr catalyst dissolved, yielding a green solution. After another 10 min, MBP was then added via a syringe. The flask was tightly sealed with a septum and dipped in an oil bath at 65 °C. After a certain length of time, samples were cooled immediately in an ice/water bath and opened to air. Then, the solution was diluted with THF and passed through a short column that was packed with silica gel and neutral alumina for complete removal of the catalyst. Solutions were then precipitated twice in a large excess of 50:50 water:methanol solution with vigorous stirring. Precipitates were collected using a centrifuge and vacuum-dried to yield light-yellow liquids. Degree of polymerization (DP) values, as tabulated in Table 1, were determined via end-group analysis of NMR spectra (using methyl groups from the initiator versus polymer backbone protons) and from SEC M_n values.

Preparation of P*n*BA-*b*-PHEA and P*n*BA-*b*-PHEMA Diblock Copolymers. The macroinitiator was dissolved in a 50:50 acetone:methanol (v/v) mixture in a round-bottom flask, and specific amounts of HEA or HEMA monomers were then added as outlined in Table 1. The flask was sealed with a septum and purged with N$_2$ for 20 min. CuBr was then charged into the flask quickly. After 5 min, 2,2'-bipyridine solid was charged into the flask quickly, and the flask was purged again for an additional 5 min before it was put in an oil bath at 60 °C for the PHEA polymerization or room temperature for the PHEMA polymerization. After a certain length of time, samples were cooled immediately in an ice/water bath, opened to air, and diluted with THF. The brown solution changed to a green color, indicating oxidation of Cu(I) species. The solution was then gradually poured into a large amount of DI water under vigorous stirring.

Table 1. Experimental Conditions for the Synthesis of the Macroinitiators and Block Copolymers via ATRP

final sample composition[a]	T (°C)	initiator	molar ratios[b] M:I:Cu(I):L	reaction time (h)	final conversion (%)	DP[f] NMR	DP[f] SEC	SEC PDI
PnBA$_{28}$	50	MBP	33:1:1:1	24	85	28	19	1.14
PnBA$_{43}$	65	MBP	75:1:1:1	12	57	43	37	1.11
PnBA$_{90}$	65	MBP	100:1:1:1	24	90	90	73	1.10
PnBA$_{114}$	65	MBP	200:1:1:1	12	57	114	85	1.14
PnBA$_{937}$	65	MBP	2000:1:10:10	96	47	NA[d]	937	1.15
PnBA$_{28}$-b-PHEMA$_{59}$	25	PnBA$_{28}$-Br	84:1:1:2	24	70	59	62	1.29
PnBA$_{43}$-b-PHEMA[c]	25	PnBA$_{43}$-Br	22:1:1:2	24				
PnBA$_{43}$-b-PHEMA[c]	25	PnBA$_{43}$-Br	129:1:1:2	24				
PnBA$_{90}$-b-PHEMA$_{39}$	25	PnBA$_{90}$-Br	45:1:1:2	24	87	39	26	1.21
PnBA$_{90}$-b-PHEMA$_{58}$	25	PnBA$_{90}$-Br	135:1:1:2	24	43	58	39	1.24
PnBA$_{90}$-b-PHEMA$_{67}$	25	PnBA$_{90}$-Br	270:1:1:2	24	25	67	53	1.29
PnBA$_{114}$-b-PHEA$_{19}$	60	PnBA$_{114}$-Br	114:1:1:2	96	17	19	NA[e]	1.14

[a] Block lengths were determined via integration of ^{1}H NMR peaks. [b] Molar ratios represent monomer:initiator:CuBr:PMDETA. [c] The PnBA MI was partially dead while polymerizing PHEMA block. [d] The DP as determined by NMR end-group analysis was not available since the end group yielded too small of a peak in comparison to the repeating units. [e] Since the PHEA block was relatively short, SEC was run without acetic anhydride esterification yielding a PDI, but not a conclusive M_n. [f] DP values for the block copolymers correspond only to the PHEMA/PHEA block.

Table 2. Reaction Parameters for the Sulfonation of PnBA-b-PHEMA Copolymers and the Corresponding Estimated HLB Values

name	prepolymer	polymer (g)	SBA (g)	TEA (g)	HLB[a]
PnBA$_{90}$-b-SBA:PHEMA$_{39}$	PnBA$_{90}$-b-PHEMA$_{39}$	1.2	1.02	0.56	10.25
PnBA$_{90}$-b-SBA:PHEMA$_{58}$	PnBA$_{90}$-b-PHEMA$_{58}$	1.2	1.33	0.73	12.24
PnBA$_{90}$-b-SBA:PHEMA$_{67}$	PnBA$_{90}$-b-PHEMA$_{67}$	1.2	1.45	0.79	12.91
PnBA$_{28}$-b-[SBA:PHEMA$_{0.12}$-co-PHEMA$_{0.88}$]$_{59}$	PnBA$_{28}$-b-PHEMA$_{59}$	0.5	0.2	0.1	
PnBA$_{28}$-b-[SBA:PHEMA$_{0.39}$-co-PHEMA$_{0.61}$]$_{59}$	PnBA$_{28}$-b-PHEMA$_{59}$	0.5	0.5	0.25	
PnBA$_{28}$-b-SBA:PHEMA$_{59}$	PnBA$_{28}$-b-PHEMA$_{59}$	0.5	1.2	0.6	16.75

[a] HLB calculations of partially sulfonated samples were not calculated.

After the polymer settled down at the bottom, the upper blue liquid was decanted. A small amount of THF/methanol mixture was then added to the precipitate and stirred. After it was swollen or dissolved, the solution was poured into a large amount of DI water, and this purifying cycle was repeated thrice. In the last step, the polymer paste was swollen in THF and then rinsed with hexane. In this way, most of the water imbibed in the original polymer was removed and guaranteed the subsequent esterification reaction. The yellowish-white solid was collected and vacuum-dried at 45 °C for at least 2 days. The DPs of the PHEA/PHEMA blocks, as tabulated in Table 1, were calculated via comparison of NMR peak areas of the ester methylene groups of the PHEA/PHEMA block with respect to the ester methylene groups of the PnBA MI. Because of the limited solubility of PHEMA in THF,[19,20] the PnBA-b-PHEMA samples were reacted with acetic anhydride as documented in the Supporting Information before SEC analysis.[21,22] DPs calculated from changes in the SEC M_n values are also shown in Table 1.

Esterification of PnBA-b-PHEMA or PnBA-b-PHEA Copolymers. All of the esterification reactions were carried out in THF at room temperature. For a typical reaction, 1.2 g of polymer was dissolved in 25 mL of THF and purged by N$_2$ for 10 min. Once the diblock copolymer had dissolved or become swollen in the solvent, TEA (2.0 equiv to HEMA or HEA) was added. The SBA (2.0 equiv to HEMA or HEA) in about 10 mL of THF was then slowly added into the reactor with TEA as the catalyst. The solution turned turbid immediately, and the reaction was stopped after 24 h. The aqueous copolymer solutions were purified by dialysis of the crude polymer in pure water with an excess amount of NaHCO$_3$ for at least 3 days to ensure complete removal of the small molecule impurities followed by 4 days of dialysis against pure water. Vo and co-workers reported that some fraction of TEA remained complexed with the new pendent sulfonate groups.[16] It was found here that by adding NaHCO$_3$ to DI water TEA was completely removed during the dialysis. For the incompletely esterified samples, PnBA$_{28}$-b-[SBA:PHEMA$_x$-co-PHEMA$_{(1-x)}$]$_{59}$, the esterification reaction was limited by decreasing the molar ratio of SBA to

PHEMA as shown in Table 2. The degree of esterification was determined via comparing the NMR peak areas from the SBA phenyl protons with those of the unreacted PHEMA methylene groups.

Emulsion Polymerization of nBA with a Diblock Copolymer Stabilizer. All emulsion polymerization reactions of nBA were carried out batch-wise in a three-neck flask at 80 °C equipped with a condenser, mechanical stirrer, and inlets for N$_2$ and monomer. Prior to polymerization, the reaction mixture, composed of 80 g of water, 20 g of nBA, and varying amounts of surfactant, was purged with N$_2$, and a small positive pressure of N$_2$ was maintained throughout the synthesis. Then, a potassium persulfate (0.15 g) solution in water was injected into the mixture to start the reaction. All of the emulsion polymerization reactions were performed using consistent conditions with the exception of type and amount of surfactant used to stabilize the latex as shown in Table 3. The diblock copolymer, PnBA$_{90}$-b-SBA:PHEMA$_{67}$, was used as the macrosurfactant while the conventional commercial surfactant (Aerosol A-103), an anionic nonylphenol ethoxylate (NPE) surfactant, was employed for comparison purposes. After 3 h, the polymerization was stopped via the removal of the reaction vessel from heat. Final latex particles were characterized via dynamic light scattering with diameters and polydispersities recorded again in Table 3.

Results and Discussion

Synthesis and Characterization of Sulfonated Diblock Copolymers. As shown in Scheme 1, generation of the strong acid-containing diblock copolymer involved the synthesis of a diblock polymer and the postmodification of the PHEA or PHEMA blocks. The PnBA homopolymer was synthesized by ATRP. All SEC chromatograms of these homopolymers in Figure 1A revealed single symmetric peaks and narrow molecular weight distributions, indicating well-controlled chain growth during ATRP. Molecular weight was adjusted within a broad range from a 28 to nearly 1000 DP with a polydispersity index (PDI) < 1.15. Given the solubility differences between PHEA or PHEMA blocks and PnBA, it was found that two

Scheme 1. Synthesis of P*n*BA-*b*-SBA:HEMA via ATRP
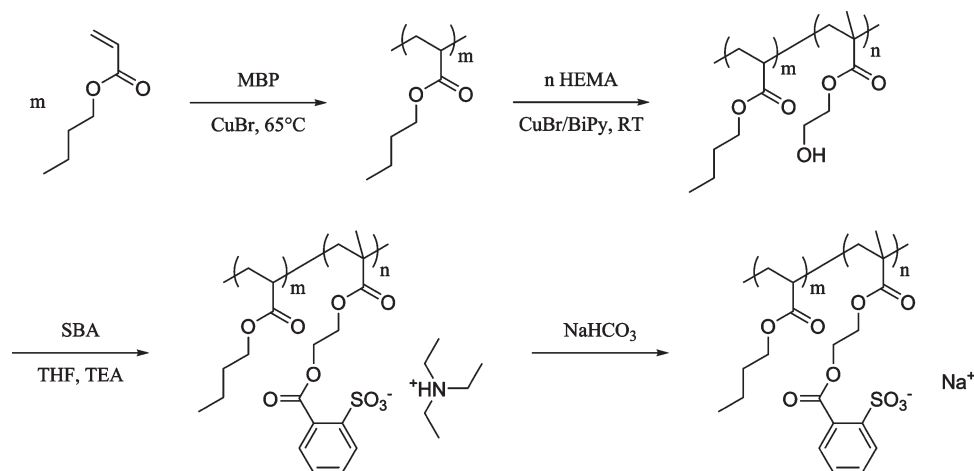
peaks appeared in the SEC traces when THF was used as the sole solvent for polymerization, as shown in Figure 1D. The peaks corresponded to the chain extended P*n*BA$_{43}$-*b*-PHEMA diblocks and unreacted P*n*BA MI. This prompted the use of a 1:1 volumetric ratio of acetone:methanol cosolvent for all other ATRP reactions of PHEA or PHEMA with P*n*BA MIs. Since ATRP of HEA monomers was fairly slow even at elevated temperatures, e.g., only 19 HEA repeating units were grown on the end of P*n*BA$_{114}$, synthesis was mainly focused on PHEMA. Although the monomers were not purified,[23] good control over MWDs was maintained, and there was no detectable residual homopolymer in the diblock copolymers as noticeable in Figure 1B, suggesting a high initiating efficiency from the P*n*BA MI.[24,25] Generally, PHEMA and PHEA homopolymers are synthesized in polar solvents such as methanol or water.[19,23,26] Alternatively, PHEMA can also be synthesized from a protected monomer like HEMA−TMS in a nonpolar solvent and deprotected after its polymerization.[27−29] As shown in Figure 1B, SEC traces of P*n*BA$_{90}$ and P*n*BA$_{90}$-*b*-PHEMA with different PHEMA lengths are given, indicating an increase in molecular weight while the individual chromatograms each retain a single elution peak with PDI < 1.3.

When the crude P*n*BA-*b*-PHEMA solution was passed through a silica gel column, the eluent remained a deep brown color, suggesting that silica gel could not effectively remove the copper species from the polymer. Because of the moderate solubility of PHEMA in water, the crude diblock copolymers were precipitated into water and copper catalysts were partially extracted into the water phase. By repeating the dissolution/precipitation process, most of the catalysts were removed. It should be noted that even though some of the final products exhibited a faint green color, it did not interfere with the subsequent esterification reactions, and ultimately the copper species were completely eliminated through extensive dialysis.

All SEC chromatograms of the diblock copolymers shown in Figure 1B,C for P*n*BA-*b*-PHEMA and P*n*BA-*b*-PHEA, respectively, revealed a single symmetric peak and narrow molecular weight distributions, indicating well-controlled chain growth during ATRP. Molecular weights as determined by SEC were found to be higher than that determined from NMR spectra, which was also found by other researchers.[19,20]

Sulfonation reactions were conducted following the method described by Vo et al. encompassing esterification of PHEMA segments.[16] For fully sulfonated samples, originating from the P*n*BA$_{90}$-*b*-PHEMA species, a 2:1 molar ratio of SBA to

−OH groups was employed to ensure complete conversion to P*n*BA$_{90}$-*b*-SBA:PHEMA as outlined in Table 2. The reaction was carried out at room temperature in the presence of the catalyst, TEA, for 24 h. As SBA was added, the diblock copolymer precursor turned turbid in minutes, and precipitation of the polymer occurred for diblock copolymers with longer PHEMA segments. Even though there was no evidence regarding the MWD of the final block copolymer, it was reasonably assumed that the PDI should have been as narrow as the precursor based on the results of Vo et al., which indicated that the esterification reaction did not change the PDI of their SBA:PHEMA homopolymers.[16]

Following the reaction, the crude product was dialyzed against an aqueous NaHCO$_3$ solution to remove small molecule impurities and TEA. The remaining electrolytes may have interfered with surface tension measurements, and therefore polymers were further dialyzed against pure water. After dialysis, purified products were obtained as polymer aqueous solutions with solid contents ranging from 1 to 5 wt % determined gravimetrically. The solutions were used for characterization by TEM, DLS, and tensiometry. Solid samples for use in NMR studies were obtained via vacuum drying at 45 °C for a minimum of 3 days.

Assigned ^{1}H NMR spectra for P*n*BA$_{90}$ MI, P*n*BA$_{90}$-*b*-PHEMA$_{67}$ diblock copolymer, P*n*BA$_{90}$-*b*-SBA:PHEMA$_{67}$ diblock copolymer crude product dialyzed against pure water, and a P*n*BA$_{90}$-*b*-SBA:PHEMA$_{67}$ diblock copolymer dialyzed against an aqueous NaHCO$_3$ solution are shown in Figure 2. The molar *n*BA:HEMA ratio was determined to be 1.33, based on integration of the ester methylene peaks of P*n*BA (h) and methylene peak groups in PHEMA (e′).

As expected, a group of peaks at $\delta = 7.3$ to 7.7 emerged after esterification corresponding to phenyl protons (a). Accordingly, methylene groups at $\delta = 3.58$ and 3.88 (e′ and e, respectively) shifted upfield to 4.26 and 4.10 (g′ and g), respectively, after the esterification reaction. The NMR spectra indicated that the reaction was complete in the P*n*BA$_{90}$-*b*-PHEMA sample series, and as can be seen, no HEMA methylene peaks (e′) were detected on NMR curves C and D. Also, the disappearance of both TEA peaks at $\delta = 1.09$ and 2.98 from Figure 2C,D indicated that NaHCO$_3$ efficiently removed the TEA, having replaced the protonated TEA with Na$^+$ ions.

In another series of samples stemming from P*n*BA$_{28}$-*b*-PHEMA$_{59}$, the degree of esterification was adjusted as can be seen from Table 2 with ^{1}H NMR results of the final
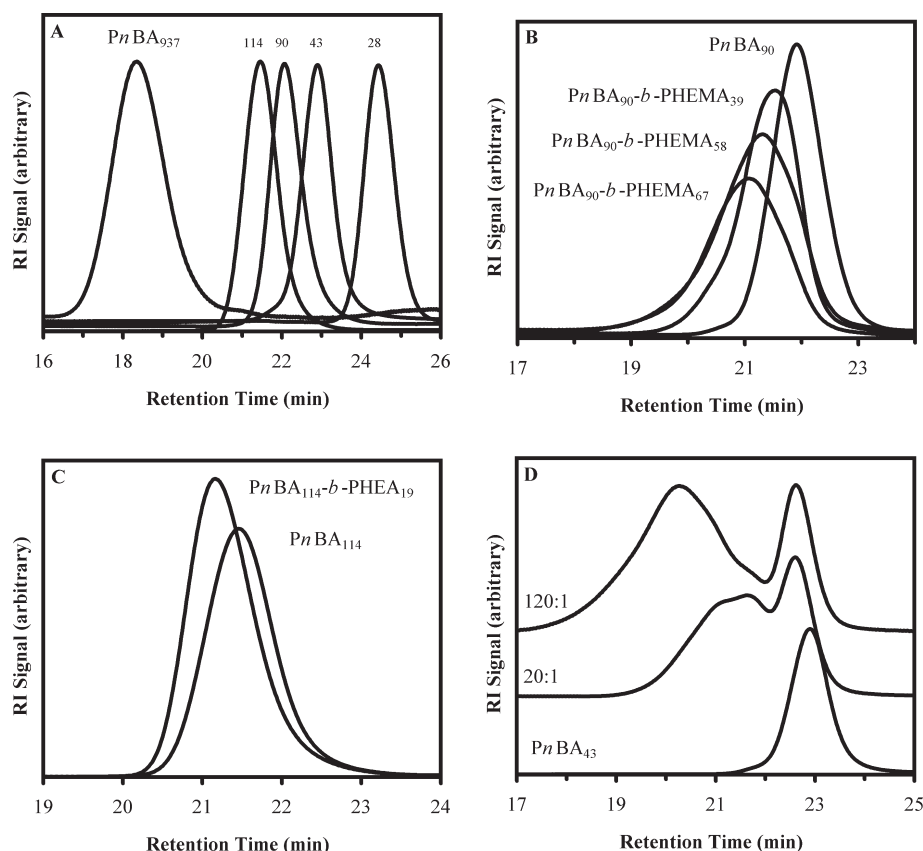
Figure 1. SEC eluograms of the P*n*BA macroinitiators and of the corresponding diblock copolymers. (A) From right to left: P*n*BA homopolymer with repeating unit of 28, 43, 90, 114, and 937, respectively. (B) From right to left: P*n*BA$_{90}$ MI, diblock copolymer with PHEMA repeating units of 39, 58, and 67, respectively. (C) P*n*BA$_{114}$ MI and P*n*BA$_{114}$-*b*-PHEA$_{19}$. (D) From bottom to top: P*n*BA$_{43}$ MI, P*n*BA$_{43}$-*b*-PHEMA using 20:1 [M]:[I], P*n*BA$_{43}$-*b*-PHEMA using 120:1 [M]:[I] ATRP conditions as shown in Table 1.
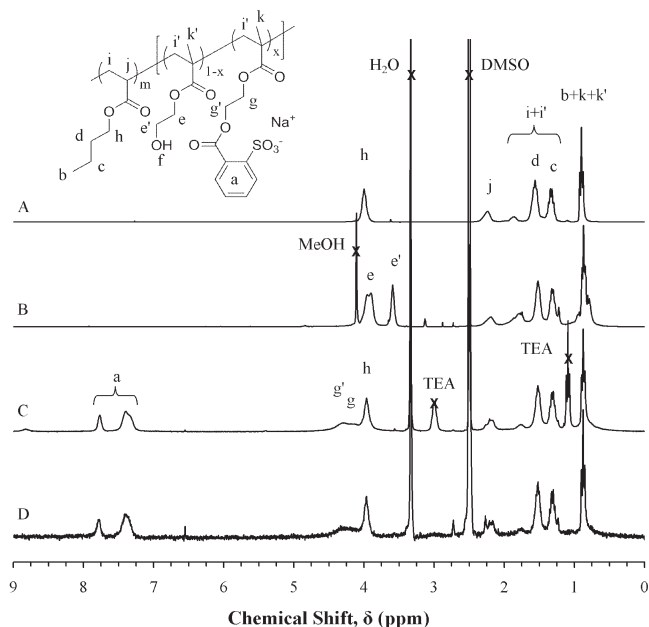
Figure 2. ^{1}H NMR spectra of P*n*BA$_{90}$-*b*-SBA:PHEMA$_{67}$ at different stages of preparation. From top to bottom the spectra were taken: (A) P*n*BA$_{90}$ MI in CDCl$_3$, (B) P*n*BA$_{90}$-*b*-PHEMA$_{67}$ in d_6-DMSO/CD$_3$OD, (C) P*n*BA$_{90}$-*b*-SBA:PHEMA$_{67}$ dialyzed against water in d_6-DMSO, and (D) P*n*BA$_{90}$-*b*-SBA:PHEMA$_{67}$ dialyzed against an aqueous NaHCO$_3$ solution in d_6-DMSO.

products shown in Figure 3. The ratio between esterified and unreacted HEMA units was calculated using the ratio of

phenyl protons (a) to those of the methylene group (e′) at $\delta = 3.58$. Alternatively, it was also obtained using the comparison of the −OH groups (f) at $\delta = 4.8$ with the phenyl protons. Both methods yielded close results, and the degree of sulfonation was calculated to be 12, 39, and 100%, respectively. Expectedly, the −OH protons disappeared for the 100% esterified sample, as shown in spectrum C.

The sulfonated diblock copolymers and their corresponding diblock and homopolymer precursors were characterized by confocal Raman microscopy. The spectra for the P*n*BA$_{90}$ MI, the intermediate diblock copolymer P*n*BA$_{90}$-*b*-PHEMA$_{67}$, and the final P*n*BA$_{90}$-*b*-SBA:PHEMA$_{67}$ diblock copolymer are shown in Figure 4. For the MI, the symmetrical Raman scattering peak at 1735 cm^{-1} reflected the presence of its ester carbonyl group. After the polymerization of the PHEMA block, a shoulder at a lower wavenumber (identified with an arrow) appeared on the carbonyl group's peak, yielding an asymmetric peak for all of the diblock copolymers. As described in a previous publication, the stretching mode of the ester carbonyl group of the acrylate species has a scattering at 1735 cm^{-1}, and the phenyl group portrays scattering at 1595 cm^{-1}.[17] The latter is therefore a characteristic scattering of SBA:PHEMA segments. Scattering by sulfonate groups at 1090 cm^{-1} could also have been used to confirm the conversion of PHEMA segments into SBA:PHEMA, but the close proximity of neighboring peaks disturbs the resolution required for a confident characterization.[30]

Micellization of Diblock Copolymers in Water. Amphiphilic block copolymers may self-assemble in selective solvents into a wide range of supramolecular structures such as
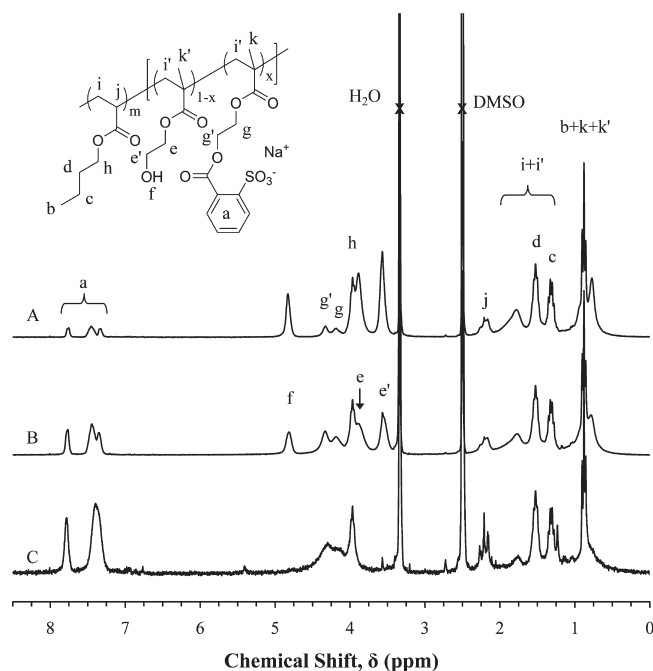
Figure 3. ^{1}H NMR spectra of sulfonated $PnBA_{28}$-SBA:PHEMA$_{59}$ at different degrees of sulfonation: (A) 12%, (B) 39%, and (C) 100% sulfonation.
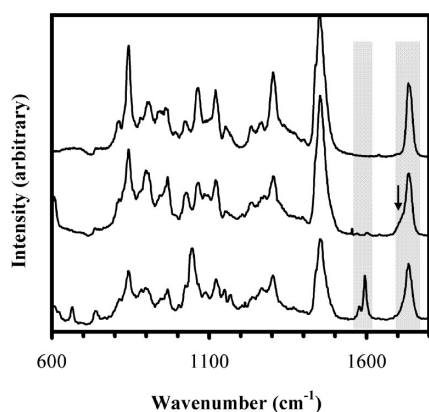

Figure 4. Raman spectra of sulfonated diblock copolymer samples and some of their precursors. From top to bottom: $PnBA_{90}$, $PnBA_{90}$-b-PHEMA$_{67}$, and $PnBA_{90}$-b-SBA:PHEMA$_{67}$. Assigned phenyl and ester carbonyl functional groups associated with the 1595 and 1735 cm^{-1} scattering peaks, respectively, are outlined with gray boxes. All of the intensities have been normalized with respect to their ester carbonyl peaks for an easier comparison.

spherical micelles, cylinders, or even gyroids. They are of interest in a number of fields for their uses in drug delivery, water purification, and stabilization of emulsion polymerization.[31,32] Morphologies of block copolymers have been reported extensively in the literature and can generally be tailored by varying the relative length (or volume fraction) of each block. However, only a few papers have reported morphologies for micelles made from strong acid block copolymers, and they are exclusively spherically shaped in water.[12,33] In comparison, there are numerous reports on the morphology study in the solid state.[34] In the present work, various micelle morphologies, including monodispersed spheres, short cylinders, and cylinder superstructures were found, depending on the relative lengths of the block segments.
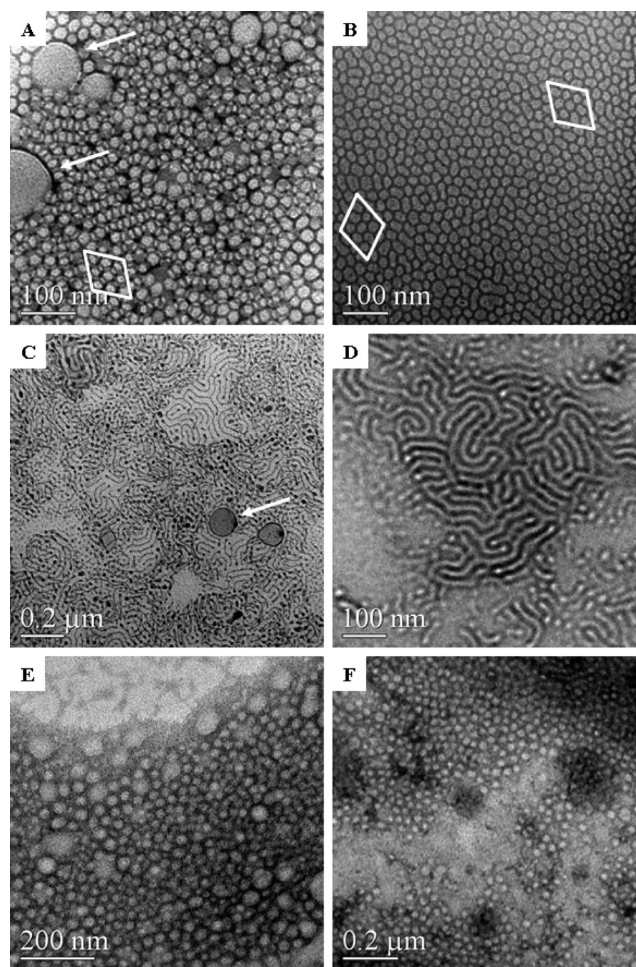

Figure 5. TEM images of the synthesized diblock copolymers stained with PTA or uranyl acetate: (A, B) $PnBA_{90}$-b-SBA:PHEMA$_{67}$ stained with PTA and uranyl acetate, respectively; (C, D) $PnBA_{90}$-b-SBA: PHEMA$_{39}$ stained with PTA at low and high magnifications; (E) $PnBA_{28}$-b-[SBA:PHEMA$_{0.12}$-co-PHEMA$_{0.88}$]$_{59}$ stained with PTA; (F) $PnBA_{28}$-b-SBA:PHEMA$_{59}$ stained with PTA.

TEM was used to follow the size and shape of the formed micelles, and several typical morphologies are given in Figures 5 and 6. PTA was the predominant stain used for TEM sample prep, but uranyl acetate was also used in place of PTA when additional insight into the micellar structure was required. For $PnBA_{90}$-b-SBA:PHEMA$_{67}$, TEM imaging revealed rather monodispersed micelles were formed through self-assembly of diblock copolymers (Figure 5A, B). The diblock copolymer formed easily recognizable spherical micelles with a diameter about 30 nm when stained with PTA. Most spheres were of the same size except for some large aggregates, identified with white arrows in Figure 5A, above 100 nm in diameter. Small spheres formed hexagonally packed arrays in some areas as indicated by the white diamonds. Regarding the composition of the larger particles, there are two possibilities: they could have been aggregates of smaller particles or vesicles. The former is more likely due to the low glass transition temperature of $PnBA$ blocks allowing for the "mobile" core to coalesce at room temperature. One might argue that the large particles could have originated from $PnBA$ homopolymer engulfed micelles. However, this possibility is inconsistent with the well-defined SEC traces of the block copolymer, and as indicated by other researchers, the introduction of homopolymers into block copolymers will cause the simultaneous swelling of all the
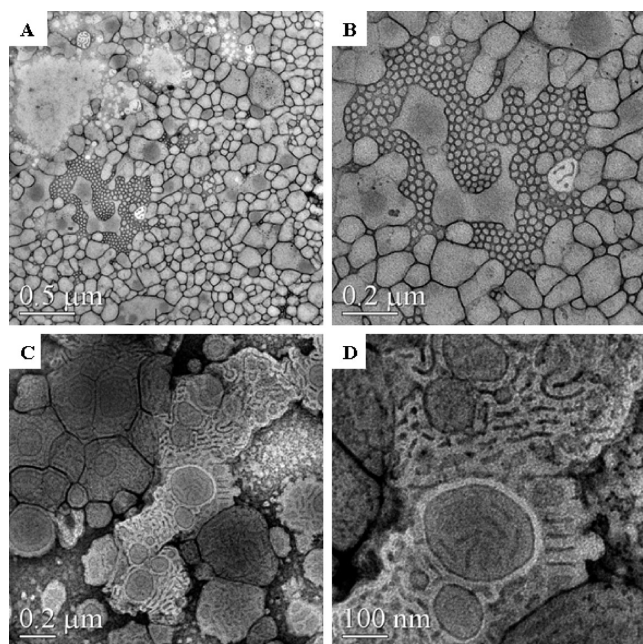
Figure 6. TEM images of $PnBA_{114}$-*b*-SBA:PHEA$_{19}$ diblock copolymer: stained with PTA at low (A) and high (B) magnifications; stained by uranyl acetate at low (C) and high (D) magnifications.

particles, provided that the homopolymer was thoroughly mixed with the block copolymer.[35] The sizes and shapes of micelles imaged were similar when stained with uranyl acetate, as shown in Figure 5B. It should be noted this sample was filtered through a 0.45 μm membrane, removing the large particles.

The dominant morphology for $PnBA_{90}$-*b*-SBA:PHEMA$_{39}$ diblock copolymer micelles were short cylinders with a diameter of ~20 nm, as shown in Figure 5C,D. Again, some large particles with diameters above 100 nm can be seen. Transitions from spherical to cylindrical morphologies as hydrophilic segments are shortened have been well documented for some block copolymers but should be associated with the lowest thermodynamic stability of diblock copolymers.[35−38] This appears to be the first reported visual inspection of cylinder micelles formed by sulfonated diblock copolymers.

For the more hydrophilic polymer with longer SBA: PHEMA segments, $PnBA_{28}$-based diblock copolymers were found to exhibit spherical micelle morphologies in all cases, as demonstrated in Figure 5E,F. Spherical micelles are a typical morphology for asymmetric block copolymers with longer hydrophilic segments.[35,37−39] Other than the large aggregates, the sizes of the smaller micelles were around 25 nm for $PnBA_{28}$-*b*-[SBA:PHEMA$_{0.12}$-*co*-PHEMA$_{0.88}$]$_{59}$ and around 30 nm for the $PnBA_{28}$-*b*-SBA:PHEMA$_{59}$ diblock copolymer, as shown in Figure 5E,F, respectively. The latter exhibited larger particle sizes probably due its more hydrophilic corona. Also, the completely esterified copolymer sample had more expanded coil conformations than its corresponding partially sulfonated counterpart.

As the hydrophobic block became significantly longer than the hydrophilic block, such as in the case of $PnBA_{114}$-*b*-SBA:PHEA$_{19}$, the PTA-stained TEM samples showed morphologies dominated by large irregularly shaped polydisperse aggregates ranging from 50 to 500 nm, as shown in Figure 6A,B. The PTA stain apparently did not penetrate the surface of the agglomerates and therefore provided no distinguishable contrast within the particles. Employment

of uranyl acetate as the TEM sample stain yielded this vital information as can be seen in Figure 6C,D. Negative staining of uranyl acetate allowed for easy identification of large aggregates composed of detailed cylindrical structures. The staining mechanisms appear to include two processes: first, uranyl acetate can form an insoluble salt with sodium ions (in contrast to the vast majority of sodium salts being water-soluble).[40,41] Second, it can also selectively bond with the anionic, particularly sulfonate, functional groups in the block copolymer micelles. The formation of such micellar aggregates has been found in other block copolymer systems and interpreted as the formation of micellar clusters. By careful inspection of the image, one can see composing cylinders are virtually interconnected or coalesced, which suggests that these cylindrical aggregates originated from different mechanisms than loose micellar clusters (LMCs). For example, in poly(styrene-*b*-ethylene oxide), the formation of LMCs was attributed to the association of poly-(ethylene oxide) chains involving hydrogen bonding between water and the polymer chains and the hydrophobic effect.[42] An additional mechanism was reported for poly(styrene-*b*-*N*-ethyl-4-vinylpyridinium bromide) where the LMCs were attributed to the presence of van der Waals attractive interactions between the micelle corona and the core.[43] In the present case, formation of the micellar clusters is considered to be due to the low glass transition temperature of the $PnBA$ core, which most likely coalesced at room temperature in solution and/or during the TEM sample preparation.

The aggregation behavior of the various copolymers in an aqueous environment was studied preliminarily by dynamic light scattering (DLS) and correlated to the results obtained by TEM. It is important to underline that DLS analysis provided only apparent values of D_h, i.e., the aggregate size of the equivalent compact sphere. Before measurement, a solution of $PnBA_{90}$-*b*-SBA:PHEMA$_{67}$ (0.1 wt %) was filtered through a 0.45 μm PVDF Millipore filter in order to remove the dust and larger micelles as appeared in Figure 5A. The DLS result is illustrated in Figure 7A with an average D_h of 78 nm. Figure 7C shows a TEM micrograph of the same sample as shown in Figure 5B while under low magnification. As can be seen, the particle size is very uniform over the whole area. The histograph distribution, as plotted in Figure 7A, was based on 200 sampled particles and yielding an average diameter of about 30 nm. Therefore, the particle size as determined by DLS is nearly twice that which is determined by TEM observation. The inconsistency between these two measurement methods was most likely due to the shrinkage of the SBA:PHEMA corona in the dry state as compared with its fully stretched state in aqueous solution, considering the strong polyelectrolytic nature of the corona.

All of the other four spherical micelles were characterized by DLS, and the results are shown in Figure 7B. The average D_h values ranged from 76 to 97 nm, which exhibited similar trends as $PnBA_{90}$-*b*-SBA:PHEMA$_{67}$. The large micelle sizes may also have originated from the aggregation of micelles. As reported in the literature, for strong polyelectrolyte micelles, the aggregation state may be influenced by several factors including the ionic strength of the aqueous medium, screening the electrostatic repulsions within the corona,[13,44,45] and the kinetics of micellar formation.[46] During the dialysis process, the conversion of solvent from THF to water accompanied by the inversion of the core−corona structure may have caused a kinetically locked structure.

Surface Tension of Amphiphilic Block Copolymer Aqueous Solutions. The surface tensions, γ, of aqueous solutions of synthesized amphiphilic diblock copolymers and the
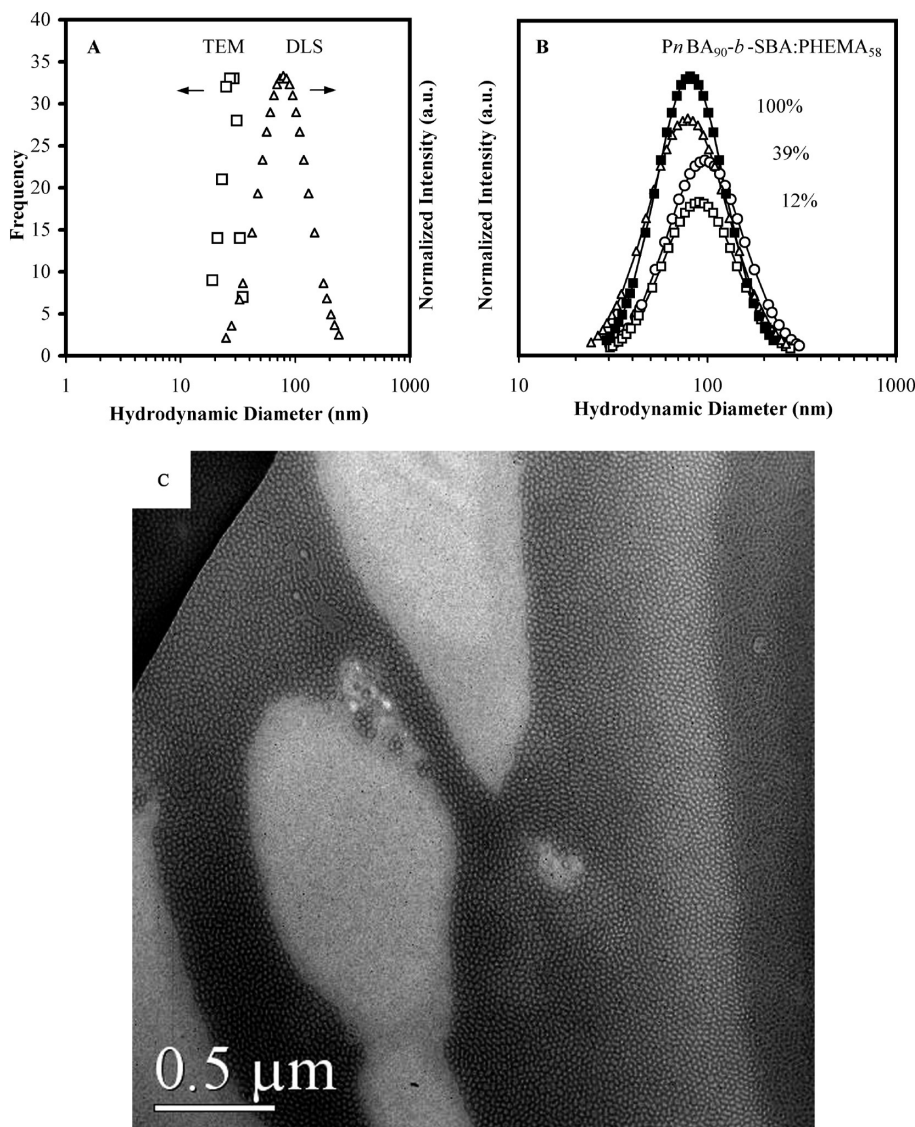
Figure 7. TEM histographs and DLS hydrodynamic diameters of block copolymer micelles. (A) Histographs of TEM and DLS derived particle size distributions for PnBA$_{90}$-b-SBA:PHEMA$_{67}$. (B) DLS of micelle hydrodynamic diameters of PnBA$_{90}$-b-SBA:PHEMA$_{58}$ (■) and three PnBA$_{28}$-b-PHEMA$_{59}$ with degrees of sulfonation at 12% (□), 39% (○), and 100% (△). (C) TEM micrograph of PnBA$_{90}$-b-SBA:PHEMA$_{67}$ micelles at low magnification.

reference NPE surfactant were measured as described above. Prior to measurements, low molar-mass impurities such as the TEA catalyst and sodium bicarbonate salt were removed from synthesized copolymers as they could strongly modify the surface tension of aqueous solutions. Removal of TEA was verified by NMR and residual NaHCO$_3$ was removed by extensive dialysis against DI water (MWCO: 2000) for at least 1 week.

Figure 8 illustrates the behavior of the synthesized diblock copolymers based on the PnBA$_{90}$ MI with varying SBA: PHEMA hydrophilic block lengths. Their limiting surface tensions grouped around 52 mN/m, with only a slight decrease in surface tension as the hydrophilic block length was increased. Independent of the hydrophilic block lengths, samples appeared to have similar critical micelle concentration (cmc) values near 5×10^{-5} mol/L, leaving the limiting surface tensions substantially higher than that of the commercial reference surfactant, but cmc values slightly lower. It should be noted that, approaching 10^{-2} mol/L, polymer solutions were viscous, which inhibited the testing of higher concentrations. These observations are in agreement with previous literature involving PnBA-b-PAA where PAA lengths ranged from 100 to 300 repeating units and the diblock copolymers showed negligible dependence of surface activity, defined here as the ability of an additive to decrease the surface tension of pure water, on their hydrophilic block lengths.[24] In fact, the limiting surface tensions are quite similar to the literature values for the case of poly-(n-butyl acrylate)-*block*-poly(2-acrylamido-2-methylpropanesulfonic acid) (PnBA-b-PAMPS).[33] Although, it should be noted that cmc values for the PnBA-b-PAMPS were calculated using their mass concentrations whereas results shown here were calculated using molar concentrations of PnBA-b-SBA:PHEMA. Considering the molecular weight differences of SPA:PHEMA blocks, the surface activities of the present diblock copolymers are actually higher for polymers with shorter SBA:PHEMA segments. This finding is consistent with the case of PnBA-b-PAMPS. Interestingly, measured cmc values were about 2 orders higher than those of PnBA-b-PAA with similar PnBA block lengths. This is likely due to the lower hydrophilicity of PAA as compared to the sulfonated copolymer. This behavior resembles the
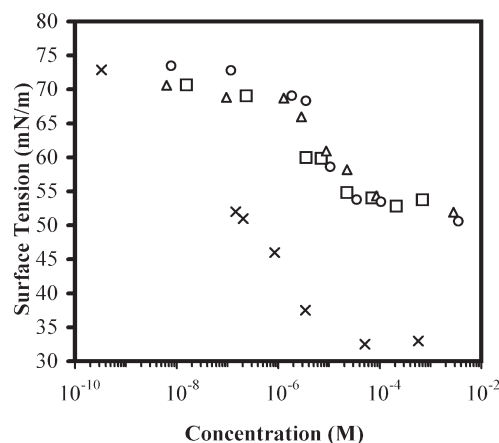
Figure 8. Surface tension vs concentration of PnBA$_{90}$ block copolymers in water with SBA:PHEMA of different segment lengths: PnBA$_{90}$-SBA:PHEMA$_{39}$ (□), PnBA$_{90}$-SBA:PHEMA$_{58}$ (○), PnBA$_{90}$-SBA:PHEMA$_{67}$ (△), and NPE (×).

Figure 9. Surface tension vs concentration of PnBA$_{28}$-b-SBA:PHEMA$_{59}$ block copolymers in water with different sulfonation levels, namely 12% (□), 39% (○), and 100% (△) sulfonated, respectively. The commercial NPE surfactant (×) is provided for comparison.

comparison between conventional anionic and nonionic surfactants, where the latter usually has a much lower cmc. The starting point of the cmc was consistent with the turbidity change of the solution at about 10^{-5} mol/L, above which solutions exhibited a blue tint color, corresponding with the formation of copolymer micelles.

For comparison, NPE as a conventional surfactant was also measured. As shown in both Figures 8 and 9, it exhibited a continuous decrease of γ with the concentration until the concentration above the cmc remained constant. Analysis of these data indicates a cmc of about 2.0×10^{-4} mol/L or 0.017 wt %, in agreement with the vendor literature.

The influence of the hydrophilicity of hydrophilic blocks was investigated using a highly controlled sample set, all prepared as described above from the PnBA$_{28}$-b-PHEMA$_{59}$ sample, with various degrees of sulfonation, namely 12%, 39%, and 100% as determined by the integration of the ^{1}H NMR peaks. PHEMA has a limited solubility in water,[47] and thus, hydrophilicity of the resulting [SBA:PHEMA$_x$-co-PHEMA$_{(1-x)}$]$_{59}$ blocks were expected to increase along with the degree of sulfonation, x. Use of this sample set allowed for a gradual increase in hydrophilicity while isolating other factors that may have influenced surface tension values such as differences in both block lengths between individual samples. Differences in the surface tension vs concentration plots of the three diblock copolymers within this sample set are obvious, as can be seen in Figure 9. The observed surface activity of the diblock copolymers was found to decrease with increasing degrees of sulfonation. For example, surface tensions around the concentrations of 10^{-2} M were 38.6, 46.8, and 49.1 mN/m as the degree of sulfonation for the diblock copolymers was increased from 12% to 39% to 100%, respectively. This trend is consistent with what others have reported in that the hydrophilicity is controlled solely by the types of monomers being used.[33] This trend is believed to be associated with the solubility of the polymer in water. While surface tension is not solely dependent upon the surface concentration of additives, all other parameters being equal, surface concentration increases as hydrophobicity of the additive is increased which can explain the change in surface tensions.

Emulsion Polymerization of nBA with Synthesized Diblock Copolymers as Emulsifiers. With the advent of controlled radical polymerization, the synthesis of amphiphilic diblock copolymers has been greatly simplified.[48] Several researchers have investigated the application of block copolymers as
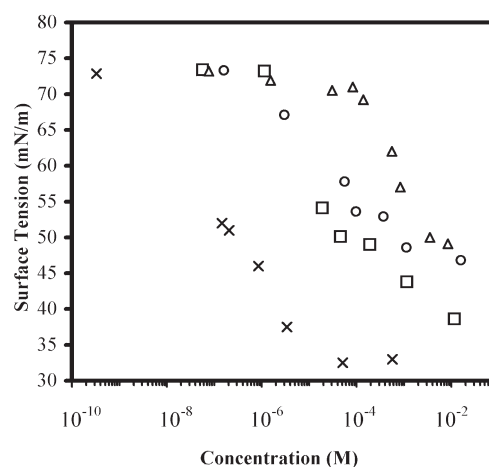
stabilizers in emulsion polymerizations of low solid latexes and non-poly(ethylene glycol)-based block copolymers, but the most heavily studied polymers bear poly(ethylene oxide) or poly(acrylic acid) (PAA) as the hydrophilic block.[8,49,50] Interesting aspects of such research include the latex particle size as a function of surfactant amount, reaction kinetics, and particle stability. Previous research indicated that such (strong acid) polymeric surfactants can effectively enhance the stability of latexes at high ion strength, which proved to be an advantage over its pH-dependent PAA counterpart.[8,31] The scope of this paper includes only aspects of the final latex particle stability, size, and distribution as a function of the amount of a PnBA-b-SBA:PHEMA block copolymeric surfactant used during emulsion polymerization.

In order to evaluate the synthesized diblock copolymer as a macrosurfactant, batch emulsion polymerizations were conducted and compared with those using the conventional NPE surfactant. Unlike conventional ionic surfactants, whose hydrophilic−lipophilic balance (HLB) values can be calculated based on HLB numbers of their encompassing functional groups (Davies' method[51]), the HLB values for synthesized macrosurfactants such as the diblock copolymers synthesized here cannot be estimated in the same manner. Using Griffin's method,[52] adopted from the literature, approximate HLB values can be estimated from the composition of the polymeric surfactants, according to the equation

$$HLB = \frac{W_H}{W_H + W_L} \times 20 \qquad (1)$$

with W_H and W_L being the weight fractions of the hydrophilic and lipophilic segments, respectively.[33,53] According to this method, HLB values of the synthesized diblock copolymers, as reported in Table 2, varied expectedly from 10.25 for the PnBA$_{90}$-b-SBA:PHEMA$_{39}$ sample with the smallest hydrophilic block length to 16.75 for the fully sulfonated PnBA$_{28}$-b-SBA:PHEMA$_{59}$ sample, which also had the largest relative hydrophilic block length. It should be noted that HLB estimates of partially sulfonated copolymers were not included since the hydrophilicity of PHEMA segments were ill-defined. Typically, surfactants with HLB values in the range of 8−18 stabilize O/W emulsions.[54] Accordingly, all fully sulfonated copolymers in the present work certainly fell within the range of HLB values suitable for emulsion polymerization.

Table 3. Experimental Conditions and Results for the Emulsion Polymerization of *n*BA Using Conventional NPE Surfactant and Synthesized Diblock Copolymeric Macrosurfactant as Stabilizers

surfactant used	surfactant amount (g)	conversion[b] (%)	particle diameter	
			nm	PD
macro[a]	0.01		310[c]	0.04
macro[a]	0.05	99.0	260	0.005
macro[a]	0.25	94.7	210	0.10
macro[a]	1.00	93.1	200	0.08
NPE	0.01		236[c]	0.18
NPE	0.05	94.1	120	0.20
NPE	0.40	91.8	71	0.20

[a] Macro represents the use of P*n*BA$_{90}$-*b*-SBA:PHEMA$_{67}$ as the stabilizer. [b] Conversion percentages measured via gravimetric experiments. [c] Denotes that aggregation occurred and therefore subsequent conversion percentages were not reported.
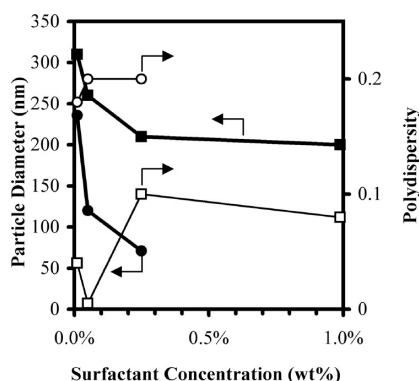

Figure 10. Emulsion particle diameters (closed symbols) and polydispersities (open symbols) using the synthesized P*n*BA$_{90}$-*b*-SBA:PHEMA$_{67}$ as emulsion surfactant (■ and □, respectively) and reference NPE surfactant (● and ○, respectively). Emulsion polymerizations of *n*BA were conducted at 80 °C for 3 h.

Figure 11. Dependence of the number density of the latex particles upon the surfactant concentration (mol/L) when using P*n*BA$_{90}$-*b*-SBA: PHEMA$_{67}$ (□) and NPE (○) as the emulsion stabilizer.

For emulsion polymerization reactions, P*n*BA$_{90}$-*b*-SBA: PHEMA$_{67}$ with its estimated HLB value of 12.9, was chosen as a stabilizer. Final latex diameters and polydispersities, as determined by DLS, are included in Table 3 and plotted as a function of surfactant concentration (wt % relative to emulsion) in Figure 10. For comparison purposes, latex particle information using the commercial NPE as the stabilizer is also included. As one can see, particle size decreased sharply from 236 to 71 nm as the amount of conventional surfactant increased from 0.010 to 0.25 wt % (0.050 to 1.2 wt % relative to monomer). Comparatively, the impact of the block copolymer concentration on particle size was much less significant; only a slight decrease from 310 to 200 nm particle diameters resulted as its concentration was increased from 0.010 to 0.99 wt % (0.05 to 4.8 wt % relative to monomer). Interestingly, Walther et al. reported the use of Janus particles (a superstructure of block copolymers) as a stabilizer for emulsion polymerizations of *n*BA.[55] Similar to the results presented here, they found that the diameters of the latex particles decreased even less, from 390 to 330 nm, as the concentration of Janus particles increased from 0.5 to 4 wt % (relative to monomer). Also expressed in Figure 10 is the influence of the synthesized macrosurfactant's concentration on the polydispersity (PD) of the latex particles with comparison to that of the NPE surfactant. Use of P*n*BA$_{90}$-*b*-SBA:PHEMA$_{67}$ as the emulsion stabilizer kept the PD of resulting particles around half of what was found when the conventional surfactant was used.

We are interested in finding how efficiently the surfactant decreases the size of the final latex particles as its concentration
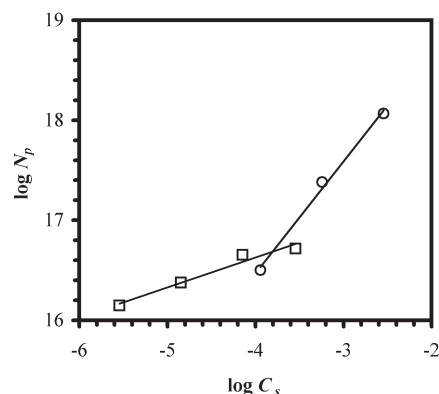
in the emulsion reaction increases. Consequently, for the same amount of surfactant, the larger the final latex particle number, and hence the smaller the particle size, the more efficient the surfactant is considered to be. At the lowest concentrations, aggregation occurred in both systems while no aggregation was observed at higher concentrations. This suggested that in the most basic sense, the polymeric surfactant was approximately as effective at stabilizing the latex particles as the reference surfactant.

One method for elucidating the effects which a surfactant has on the resulting latex particle sizes, distributions, and stability can be found in the exponent value of

$$N_p = k[C_s]^\alpha \tag{2}$$

where N_p is the number of particles per unit liter, k is an agglomeration of constants dependent upon the rate of radical generation and growth of the polymer latex volume, C_s is the molarity of the surfactant (with respect to the emulsion volume), and α is a variable (below unity) which correlates to the immobility of the surfactant in the aqueous phase of the emulsion.[48,49,56,57] Particle number densities, N_p, were calculated using the particle sizes, as determined by DLS, and the known masses of the emulsion constituents along with a density of 0.8937 g/mL from the literature for P*n*BA.[58] Linear regression was used to determine k and α from the log−log plots of the N_p dependency on C_s as shown in Figure 11 for both the macrosurfactant and NPE stabilized emulsion polymerization reactions. Of interest here are the α values, which were found to be 0.30 for the polymeric macrosurfactant and 1.1 for NPE. The α value of the present polymeric surfactant is close to values reported elsewhere of 0.40 for a P*n*BA$_9$-*b*-PAA$_{11}$ surfactant used in the polymerization of MMA/*n*BA.[48] The increase in hydrophilicity, and therefore mobility, of the P*n*BA$_{90}$-*b*-SBA:PHEMA$_{67}$ as depicted by a decreased α with respect to P*n*BA$_9$-*b*-PAA$_{11}$ is most likely due to the difference in their hydrophilic functional groups. The pK_a of sulfonate is much lower than carboxylate, allowing for a noticeable difference in the ionized fraction, and therefore the hydrophilicity, of the surfactant especially at neutral pH ranges. The unexpectedly high α value for the commercial NPE may be a result of the polydispersity of the emulsion particles skewing the slope of the log−log plot due to the method of determining the number density from the DLS results. A high α value is advantageous in the sense that all micelles are used during the nucleation process, which is preferable if a high solids latex consisting of many small particles is desired. However, with such a surfactant, latex particles may have a lower

colloidal stability due to large "bare" hydrophobic surface patches. This may account for the broader size distribution of latex particles emulsified by the commercial NPE. Investigation of these effects will be a component of a future study of the diblock copolymers generated here.

Summary and Conclusions

Sulfonated amphiphilic diblock copolymers were successfully synthesized with narrow MWDs via ATRP under relatively mild reaction conditions. Synthesis involved sequential ATRP of *n*BA and HEMA followed by the esterification of the PHEMA blocks with SBA in THF at room temperature. The versatile morphologies of the block copolymer micelles were systematically studied and cylindrical and cylindrical aggregate micellar morphologies were reported here for the first time. Surface tensions of synthesized macrosurfactant solutions were correlated to the block lengths and degrees of sulfonation of the SBA:PHEMA segments. The results indicate that surface tension has little dependency on the length of fully sulfonated SBA:PHEMA segments ranging from 39 to 67 repeating units. In contrast, the degree of sulfonation of SBA:PHEMA blocks directly affects surface activity of copolymer solutions at constant surfactant concentrations; i.e., surface tension decreases with decreasing sulfonation. A single macrosurfactant sample, P*n*BA$_{90}$-*b*-SBA:PHEMA$_{67}$, was used as the stabilizer for batch emulsion polymerization experiments. Compared with the relatively lower molecular weight commercial NPE, the diblock copolymer surfactant was less efficient in decreasing the latex particle sizes but more effective at decreasing polydispersity of the emulsion particles. It is quite possible that sulfonated diblock copolymers synthesized here could serve as a replacement for conventional lower molecular weight surfactants used during the synthesis of P*n*BA latexes.

Supporting Information Available: Procedure for acetylation of P*n*BA-*b*-PHEMA block copolymers. This material is available free of charge via the Internet at http://pubs.acs.org.

References and Notes

(1) Eisenberg, A.; Kim, J. In *Introduction to Ionomers*; Wiley: New York, 1998; pp 307−314, 327.
(2) Robinson, K. L.; Weaver, J. V. M.; Armes, S. P.; Martin, E. D.; Meldrum, F. C. *J. Mater. Chem.* **2002**, *12*, 890–896.
(3) Storey, R. F.; Baughill, D. W. *Polymer* **2000**, *41*, 3205–3211.
(4) Weiss, R. A.; Sen, A.; Willis, C. L.; Pottick, L. A. *Polymer* **1991**, *32*, 1867–1874.
(5) Ioannou, E. F.; Mountrichas, G.; Pispas, S.; Kamitsos, E. I. *Macromolecules* **2008**, *41*, 6183–6190.
(6) Leemans, L.; Fayt, R.; Teyssie, P. *J. Polym. Sci., Polym. Chem.* **1990**, *28*, 1255–1262.
(7) Liu, T.; Schuch, H.; Gerst, M.; Chu, B. *Macromolecules* **1999**, *32*, 6031–6042.
(8) Müller, H.; Leube, W.; Tauer, K.; Förster, S.; Antonietti, M. *Macromolecules* **1997**, *30*, 2288–2293.
(9) Bouix, M.; Gouzi, J.; Charleux, B.; Vairon, J.; Guinot, P. *Macromol. Rapid Commun.* **1998**, *19*, 209.
(10) Ma, Y.; Tang, Y.; Billingham, N. C.; Armes, S. P.; Lewis, A. L.; Lloyd, A. W.; Salvage, J. P. *Macromolecules* **2003**, *36*, 3475.
(11) Mitsukami, Y.; Donovan, M. S.; Lowe, A. B.; McCormick, C. L. *Macromolecules* **2001**, *34*, 2248.

(12) Masci, G.; Bontempo, D.; Tiso, N.; Diociaiuti, M.; Mannina, L.; Capitani, D.; Crescenzi, V. *Macromolecules* **2004**, *37*, 4464–4473.
(13) Garnier, S.; Laschewsky, A. *Macromolecules* **2005**, *38*, 7580–7592.
(14) Chu, C.; Wang, Y.; Yeh, C.; Wang, L. *Macromolecules* **2008**, *41*, 5632–5640.
(15) Baek, K. *J. Polym. Sci., Polym. Chem.* **2008**, *46*, 5991–5998.
(16) Vo, C. D.; Iddon, P. D.; Armes, S. P. *Polymer* **2007**, *48*, 1193–1202.
(17) Xu, G. Z. H.; Dong, J. P.; Zhang, J. G.; Severtson, S. J.; Houtman, C. J.; Gwin, L. E. *J. Phys. Chem. B* **2008**, *112*, 11907–11914.
(18) Berne, B. J.; Pecora, R. In *Dynamic Light Scattering with Applications to Chemistry, Biology, and Physics*; Dover Publications: Mineola, NY, 1976.
(19) Robinson, K. L.; Khan, M. A.; Báñez, M. V.; Wang, X. S.; Armes, S. P. *Macromolecules* **2001**, *34*, 3155–3158.
(20) Tong, X.; Zhang, X.; Ye, L.; Zhang, A.; Feng, Z. *Polymer* **2008**, *49*, 4489–4493.
(21) Clément, B.; Trimaille, T.; Alluin, O.; Gigmes, D.; Mabrouk, K.; Féron, F.; Decherchi, P.; Marqueste, T.; Bertin, D. *Biomacromolecules* **2009**, *10*, 1436–1445.
(22) Ruckenstein, E.; Zhang, H. *Polym. Bull.* **2001**, *47*, 113–119.
(23) Coca, S.; Jasieczek, C. B.; Teers, K. L.; Matyjaszewski, K. *J. Polym. Sci., Polym. Chem.* **1998**, *36*, 1417–1424.
(24) Colombani, O.; Ruppel, M.; Schubert, F.; Zettl, H.; Pergushov, D.; Müller, A. *Macromolecules* **2007**, *40*, 4338–4350.
(25) Piogé, S.; Fontaine, L.; Gaillard, C.; Nicol, E.; Pascual, S. *Macromolecules* **2009**, *42*, 4262–4272.
(26) Cai, Y.; Armes, S. P. *Macromolecules* **2004**, *37*, 7116–7122.
(27) Matyjaszewski, K.; Xia, J. *Chem. Rev.* **2001**, *101*, 2921–2990.
(28) Pietrasik, J.; Sumerlin, B.; Lee, R. Y.; Matyjaszewski, K. *Macromol. Chem. Phys.* **2007**, *208*, 30–36.
(29) Zheng, R.; Liu, G.; Jao, T. *Polymer* **2007**, *48*, 7049–7057.
(30) Belaroui, F.; Grohens, Y.; Boyer, H.; Holl, Y. *Polymer* **2000**, *41*, 7641–7645.
(31) Leemans, L.; Fayt, R.; Teyssie, P.; De Jaeger, N. C. *Macromolecules* **1991**, *24*, 5922–5925.
(32) Riess, G. *Colloids Surf., A* **1999**, *153*, 99–110.
(33) Garnier, S.; Laschewsky, A. *Langmuir* **2006**, *22*, 4044–4053.
(34) Rubatat, L.; Li, C.; Dietsch, H.; Nykänen, A.; Ruokolainen, J.; Mezzenga, R. *Macromolecules* **2008**, *41*, 8130–8137.
(35) Zhang, L.; Eisenberg, A. *J. Am. Chem. Soc.* **1996**, *118*, 3168–3181.
(36) Kaewsaiha, P.; Matsumoto, K.; Matsuoka, H. *Langmuir* **2007**, *23*, 9162–9169.
(37) Zhang, L.; Barlow, R. J.; Eisenberg, A. *Macromolecules* **1995**, *28*, 6055–6066.
(38) Zhang, L.; Eisenberg, A. *Macromolecules* **1996**, *29*, 8805–8815.
(39) Discher, D. E.; Eisenberg, A. *Science* **2002**, *297*, 967–973.
(40) Chamot, E. M.; Bedient, H. A. *Mikrochemie* **1928**, *6*, 13–21.
(41) Trinder, P. *Analyst* **1951**, *76*, 596–599.
(42) Xu, R.; Winnik, M. A.; Hallett, F. R.; Riess, G.; Croucher, M. D. *Macromolecules* **1991**, *24*, 87–93.
(43) Lysenko, E. A.; Bronich, T. K.; Slonkina, E. V.; Eisenberg, A.; Kabanov, V. A.; Kabanov, A. V. *Macromolecules* **2002**, *35*, 6351–6361.
(44) Lee, A. S.; Bütün, V.; Vamvakaki, M.; Armes, S. P.; Pople, J. A.; Gast, A. P. *Macromolecules* **2002**, *35*, 8540–8551.
(45) Lee, A. S.; Gast, A. P.; Bütün, V.; Armes, S. P. *Macromolecules* **1999**, *32*, 4302–4310.
(46) Riess, G. *Prog. Polym. Sci.* **2003**, *28*, 1107–1170.
(47) Weaver, J. V. M.; Bannister, I.; Robinson, K. L.; Bories-Azeau, X.; Armes, S. P. *Macromolecules* **2004**, *37*, 2395–2403.
(48) Gaillard, N.; Guyot, A.; Claverie, J. *J. Polym. Sci., Polym. Chem.* **2003**, *41*, 684–698.
(49) Burguière, C.; Pascual, S.; Bui, C.; Vairon, J.; Charleux, K. A.; Matyjaszewski, K.; Btremieux, I. *Macromolecules* **2001**, *34*, 4439–4450.
(50) Pincus, P. *Macromolecules* **1991**, *24*, 2912–2919.
(51) Davies, J. T. *Proc. Int. Congr. Surf. Act.* **1957**, *1*, 426–438.
(52) Griffin, W. C. *J. Soc. Cosmet. Chem.* **1954**, *5*, 259.
(53) Tan, B.; Grijpma, D. W.; Nabuurs, T.; Feijen, J. *Polymer* **2005**, *46*, 1347–1357.
(54) Tadros, T. F. In *Applied Surfactants: Principles and Applications*; Wiley-VCH Verlag: Weinheim, Germany, 2005.
(55) Walther, A.; Hoffmann, M.; Müller, A. *Angew. Chem., Int. Ed.* **2008**, *47*, 711–714.
(56) Rager, T.; Meyer, W. H.; Wegner, G.; Mathauer, K.; Mächtle, W.; Schrof, W.; Urban, D. *Macromol. Chem. Phys.* **1999**, *200*, 1681–1691.
(57) Smith, W. V.; Ewart, R. H. *J. Chem. Phys.* **1948**, *16*, 592–599.
(58) Barudio, I.; Févotte, G.; McKenna, T. F. *Eur. Polym. J.* **1999**, *35*, 775–780.